3 Biotech (2017) 7:249
DOI 10.1007/s13205-017-0889-0

ORIGINAL ARTICLE

Characterization, drug loading and antibacterial activity of nanohydroxyapatite/polycaprolactone (nHA/PCL) electrospun membrane

Mohd Izzat Hassan[1] · **Naznin Sultana**[1,2]

Received: 22 October 2016 / Accepted: 11 July 2017 / Published online: 17 July 2017

Abstract Considering the important factor of bioactive nanohydoxyapatite (nHA) to enhance osteoconductivity or bone-bonding capacity, nHA was incorporated into an electrospun polycaprolactone (PCL) membrane using electrospinning techniques. The viscosity of the PCL and nHA/PCL with different concentrations of nHA was measured and the morphology of the electrospun membranes was compared using a field emission scanning electron microscopy. The water contact angle of the nanofiber determined the wettability of the membranes of different concentrations. The surface roughness of the electrospun nanofibers fabricated from pure PCL and nHA/PCL was determined and compared using atomic force microscopy. Attenuated total reflectance Fourier transform infrared spectroscopy was used to study the chemical bonding of the composite electrospun nanofibers. Beadless nanofibers were achieved after the incorporation of nHA with a diameter of 200–700 nm. Results showed that the fiber diameter and the surface roughness of electrospun nanofibers were significantly increased after the incorporation of nHA. In contrast, the water contact angle (132° ± 3.5°) was reduced for PCL membrane after addition of 10% (w/w) nHA (112° ± 3.0°). Ultimate tensile strengths of PCL membrane and 10% (w/w) nHA/PCL membrane were 25.02 ± 2.3 and 18.5 ± 4.4 MPa. A model drug tetracycline hydrochloride was successfully loaded in the membrane and the membrane demonstrated good antibacterial effects against the growth of bacteria by showing inhibition zone for *E. coli* (2.53 ± 0.06 cm) and *B. cereus* (2.87 ± 0.06 cm).

Keywords Polycaprolactone · Hydroxyapatite · Electrospinning · Nanofiber scaffold · Antibacterial

Introduction

Using nanofibers as scaffold or membrane for replacing tissue loss can mimic the natural structure of the extracellular matrix (ECM) (Agarwal et al. 2009). The electrospinning technique is an efficient method of producing continuous and fine (micro/nano) scale fibers by drawing out the polymer solution under electrostatic forces into the whipping jets, and continuous fiber can be deposited on the conductive collector (Kim et al. 2006). Electrospinning-processing parameters such as solutions, distances between tips to collector, high-voltage supply, flow rate of injection pump and room humidity can be optimized to obtain beadless and uniform nanofibers (Chung et al. 2016). Polycaprolactone (PCL), a synthetic biodegradable polymer, is a suitable choice for bone tissue engineering application to let the scaffold stay in the human body before being substituted by new bone tissue (Leung and Ko 2011; Putti et al. 2015).

Nanohydroxyapatite (nHA), an inorganic biomaterial similar to the mineral constituent in bone, possesses excellent biocompatibility and osteoconductivity as bone substitute and is widely used in biomedical applications (Webster and Ahn 2007). However, nHA is highly brittle and has poor mechanical properties. Hence, nHA is usually

✉ Naznin Sultana
naznin@biomedical.utm.my

[1] Faculty of Biosciences and Medical Engineering, Universiti Tek nologi Malaysia, 81310 UTM Johor Bahru, Johor, Malaysia

[2] Advanced Membrane Technology Research Center, Universiti Teknologi Malaysia, 81310 UTM Johor Bahru, Johor, Malaysia

combined with biopolymer and organic material into a composite form to overcome the limitations of its mechanical properties. Many studies have been reported on the fabrication of composite scaffolds using nHA with biocompatible polymers, such as poly-L-lactic acid (PLLA) (Davachi et al. 2016), poly-L-glycolic acid (PLGA) (Zheng et al. 2013), poly(hydroxybutyrate-co-valerate) (PHBV) (Sultana and Wang 2008), cellulose (Zadegan et al. 2011), PCL (Hassan et al. 2014), and polyvinyl alcohol (PVA) (Sultana and Zainal 2016).

Biomolecules such as drugs, proteins, DNA and growth factors can be loaded into the electrospun nanofiber for drug delivery application or to inhibit infections (Kim et al. 2012). The nanofiber containing the drugs can be designed with multiple functions, such as for temporary support, drug delivery capabilities, and antibacterial properties to serve as signaling of biochemicals to the cells and avoiding infections after surgery (Pillay et al. 2013).

In this study, electrospun PCL membrane was fabricated using the electrospinning technique. nHA was incorporated into the PCL membrane to render the membrane osteoconductive. Electrospinning of nHA/PCL using acetone solvent is not frequently reported and utilized. Common solvents that have been used to dissolve PCL for fabricating PCL nanofiber are dichloromethane/dimethyl formamide (Wutticharoenmongkol et al. 2006), trifluoroethanol (Samavedi et al. 2011), methanol/chloroform (Zhang et al. 2007), methylene chloride/dimethyl formamide (Li et al. 2012), and hexafluoroethanol (Jaiswal et al. 2013). Some of these solvents are harmful and required attentive caution and safety precautions while preparing the solution for electrospinning. Utilizing acetone or a less harmful solvent is one way to avoid this problem. The influence of the addition of nHA on the microstructure and the surface roughness of PCL fibers was investigated. The nHA/PCL composite membrane was characterized using field emission scanning electron microscopy (FESEM), energy dispersive X-ray spectroscopy (EDX), atomic force microscopy (AFM), contact angle measurements and attenuated total reflectance Fourier transform infrared spectroscopy (ATR-FTIR). Tensile mechanical properties of the membrane of the nanofiber were determined. Meanwhile, tetracycline hydrochloride (TCH), a model drug, was incorporated together with nHA/PCL to study the feasibility of the antibacterial ability of the membrane to avoid bacterial infection during the surgical procedure. This paper reports our new findings on suitable properties of nHA/PCL membrane to be used in bone tissue engineering applications. The main objective of this study was to investigate the effect of the incorporation of nHA and TCH on PCL membrane and compare the morphology, wettability and surface roughness. As reported in our previous study (Hassan et al. 2014), incorporation of 10% (w/w) nHA in PCL membrane resulted in a membrane with better fiber properties; the present study will focus on morphology, wettability, mechanical analysis, antibacterial ability and drug release of nanofibers composed of pure PCL and 10% (w/w) nHA/PCL membrane.

Materials and methods

Materials

PCL with molecular weight (M_n 70,000–900,000) and acetone were supplied by Sigma-Aldrich, USA. The nHA was synthesized in-house using a nanoemulsion process described elsewhere (Zhou et al. 2008). A solution of $Ca(NO_3)_2{\cdot}4H_2O$ in acetone was mixed for 30 s with a solution of $(NH_4)_2HPO_4$ in distilled water at pH 11. The mixed solution was filtered with filter paper and washed three times using distilled water. The precipitate was frozen overnight and then freeze-dried using a freeze-drying system (Labconco, USA).

Preparation of electrospinning solutions and drug loading

PCL (0.75 g) was dissolved in acetone (10 ml) to make 7.5% (w/v) PCL solution. The weight percentage of nHA was based on the weight of the PCL. 10% (w/w) (0.075 g) of nHA was added to PCL solution to prepare 10% (w/w) nHA/PCL solutions. The nHA/PCL solutions were homogenized for 3 min using a homogenizer (IKA Works T25, Germany). To make the TCH/PCL and TCH/nHA/PCL solution, TCH had to be predissolved in methanol before adding to the solution. 0.2 g TCH was dissolved in 10 mL methanol to load 2% (w/v) TCH into the nanofibers (Chong et al. 2015). After all the TCH was completely dissolved into methanol, 1 mL of TCH solution was taken out and added to the polymer solution. Then the electrospinning was carried out to fabricate TCH/PCL and TCH/nHA/PCL membranes.

Viscosity of solutions

The viscosity of solutions was measured at room temperature using a Brookfield rotational viscometer, LVDV-II + PRO (Brookfield Engineering Labs., Inc., Middleboro, MA, USA) with an SC4-18 spindle and a torque of 0.0673 milli Newton-m. The rotational speed was 0.5 rpm.

Electrospinning

The prepared solution was transferred into a 5-ml syringe with a blunt-end 22 G needle. The solution was ejected at a feeding rate of 3 ml/h using an infusion pump (NE-300, New Era Pump Systems Inc., USA). The distance between

the needle tips to the grounded aluminum collector was kept constant at 10 cm. A high voltage of 22 kV was applied to the needle. The relative humidity of the room was in the range of 50–60%. The resulting fibers were dried overnight and stored in a desiccator prior to analysis.

Field emission scanning electron microscopy (FESEM) and energy dispersive spectroscopy (EDX)

The microstructures of the electrospun fibers were sputter-coated with gold and then observed by using a field emission scanning electron microscopy (Hitachi SU8020, Japan) at an accelerating voltage of 15 kV using secondary electron (SE) at a working distance of 15,800 μm. The diameters of resulting fibers were measured at random locations on each fiber. From the images, at least 50 measurements were calculated using image analysis software (Image J, NIH, USA) and the average diameter was measured. Energy dispersive X-ray (EDX) attached with the FESEM was used to confirm the presence of nHA in the PCL polymer solution.

Water contact angle

The wettability of the membrane was measured using a contact angle instrument (VCA Optima, USA) by dropping 2 μl of deionized water onto the membrane. The measurement was performed five times at different locations of the membrane and the average value was calculated.

Surface roughness

The roughness of the membrane's surface was acquired from an AFM (AFM, Digital Instruments, Santa Barbara, CA) at 512 scan lines with a scan size of 15 μm and a scan rate of 0.5 Hz. The root-mean-squared roughness (Rms) values determined the mean roughness of the membrane:

$$\mathrm{Rms} = \sqrt{\frac{\sum (Z_i - Z_{\mathrm{ave}})^2}{(N)}}, \quad (1)$$

where Z_{ave} is the average of the Z values within the given area and Z_i is the current Z values and N is the number of point within the given area. Five different locations of AFM images of the fibers were taken and the average value was calculated.

ATR-FTIR

The chemical bonds of nHA, PCL and nHA/PCL nanofibers were investigated using the ATR-FTIR (Perkin-Elmer Spectrometer, MA, USA). The samples were clamped to the ATR crystal. Then, the infrared spectra were recorded at (4000–650) cm^{-1} region with a resolution of 4.0 cm^{-1} and 16 scan using universal ATR sampling accessory.

Tensile mechanical properties

Tensile mechanical properties of the PCL and 10% (w/w) nHA/PCL fibers were determined using an Instron Mechanical Tester (Microtester 5848, Instron, USA) with a load cell of 10 N at a cross-head speed of 1 mm/min. Rectangular specimens (5 mm × 30 mm) fabricated from optimized parameters of PCL and nHA/PCL fibers at 10% nHA concentration were prepared. From the machine-recorded data, stress–strain relationship was obtained and the ultimate tensile strength and Young's modulus were determined from the stress–strain curve. Five specimens for each sample were examined and the results were expressed as mean ± standard deviation (SD).

Antibacterial test and drug release study

The antibacterial activity of electrospun TCH/nHA/PCL fibers was investigated using a zone inhibition method. Bacterial species (*E. coli* and *B. cereus*) were used as the model microorganisms. Using a spread plate method, nutrient agar plates were inoculated with 1 mL of bacterial suspension containing around 108 cfu/mL. The nanofiber membranes in circular disc form of 1.8 cm diameter were gently placed on the inoculated plates, and then incubated at 37 °C for 24 h. Zones of inhibition were calculated by measuring the clear area around each electrospun nanofiber samples.

The electrospun TCH-loaded membranes were cut into 2 cm × 1 cm pieces. The samples were then immersed into 10 mL phosphate buffer solution (PBS) at 37 °C. After each time interval, 1 mL of PBS was taken from the sample tubes and then the absorbance was measured using a UV spectroscopy at a wavelength of 275 nm (Koneru et al. 2015). UV–visible spectroscopy measurements were performed for known concentrations of TCH at the absorbance of 275 nm and a standard curve was constructed (Koneru et al. 2015). The amount of drug (μg) released was calculated using the standard curve of the absorbance at 275 nm. After each measurement, 1 mL of fresh PBS solution was mixed with the sample to replace the PBS solution taken from the previous step.

Results and discussion

Morphology of fibers

Nanohydroxyapatite (nHA) was produced by using the nanoemulsion freeze-drying technique. The FESEM image

of synthesized nHA and EDX spectrum are shown in Fig. 1a. Nanosphere-like nanoparticles with an average diameter of 35.12 ± 0.66 nm were observed. EDX spectrum showed the presence of Ca and P in the nHA. To fabricate electrospun nanofibers, one of the important steps is to dissolve the polymers in a suitable solvent, since this can affect the property of the solution and also prevent from using a harmful and toxic solvent. Utilizing acetone as a solvent could eliminate the risk of toxicity and has been shown to successfully fabricate nanofibers (Romeo et al. 2007). Electrospinning parameters, such as distance between the needle tips to collector, the supplied voltage, the flow rate of the syringe pump and the ambient condition of the room, were optimized at 10 cm, 22 kV, 3 ml/h, and (50–60)% relative humidity, to obtain the structure of nanofiber as shown in Fig. 1b–d. The solution of PCL that was prepared using the polymer concentration of 7.5% (w/v) had a low viscosity of 28.5 cP, which produced the thin

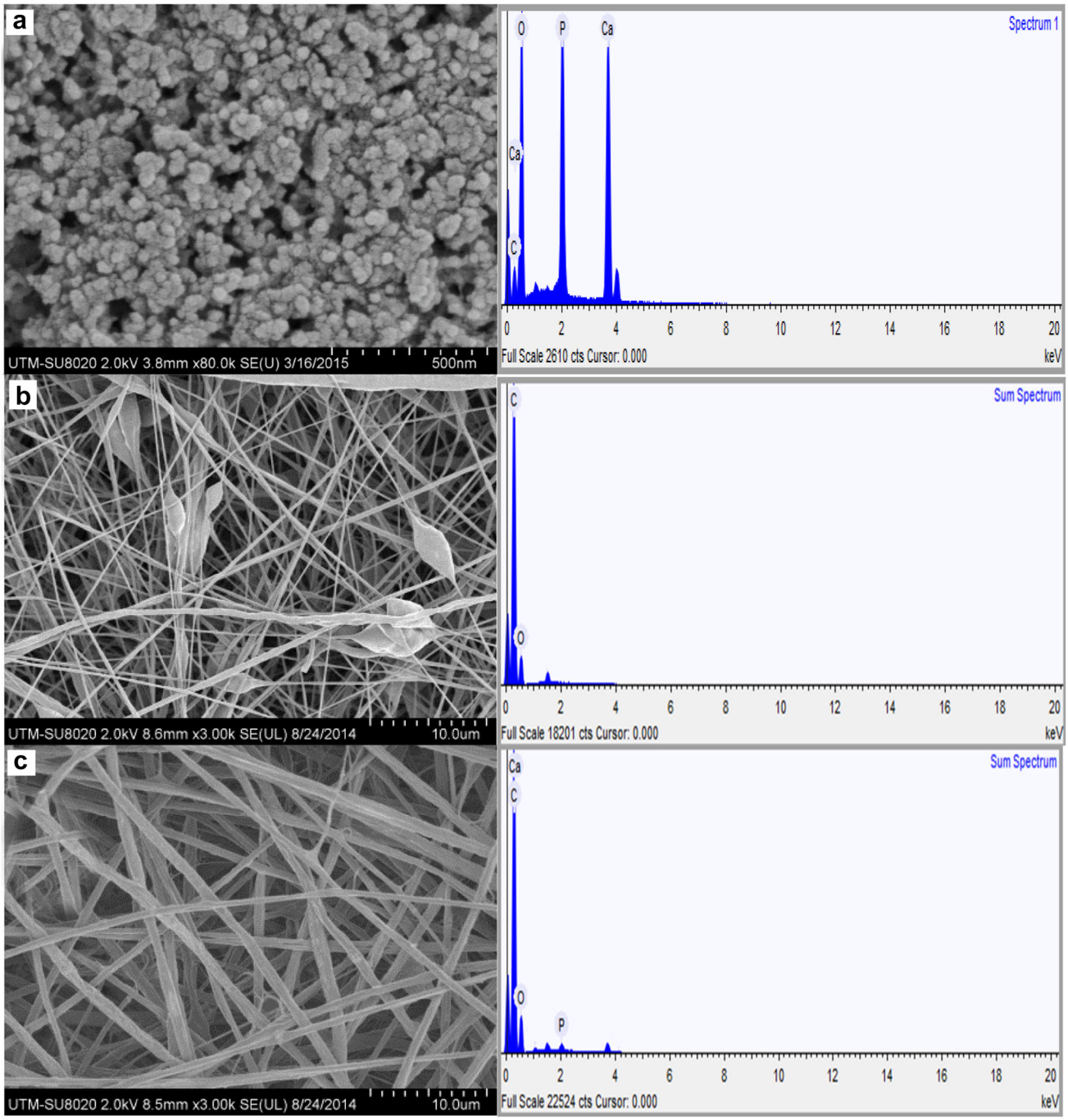

Fig. 1 FESEM micrographs (*left*) and EDX spectra (*right*) of **a** nHA nanoparticles and **b** PCL, **c** 10%(w/w) nHA/PCL electrospun fibers

nanofiber with spindle-like beads along the nanofibers (Fig. 1; Table 1). Based on our previous works, 7.5% (w/v) PCL was optimized, since a higher concentration produced an even larger diameter with non-uniform fiber morphology (Hassan et al. 2014). The average fiber diameter of PCL fiber was 0.25 ± 0.08 μm. 10% (w/w) nHA was incorporated into the same polymer solution concentration. The viscosity of the solution was increased with the incorporation of nHA particles. In addition, the beads were eliminated with the incorporation of 10% (w/w) nHA. The fiber diameter was also increased. The average fiber diameter of 10% (w/w) nHA/PCL fiber was 0.65 ± 0.18 μm (Table 1). It can be mentioned that further increasing the viscosity of the solution results in fibers with a larger diameter. The reason for this is that higher viscosity induces higher stress relaxation time and a higher chain entanglement of the polymer. These conditions prevented the jet from breaking up during the ejection of the electrospinning process solution and increased the fiber diameter (Wutticharoenmongkol et al. 2007; Sun et al. 2014). The EDX spectrum of 10% (w/w) nHA/PCL confirmed the presence of the elements of nHA (Ca and P) (Fig. 1c). Overall, the morphology of the fabricated nanofibers was controlled by the concentration and viscosity of the solution. The morphology of the fabricated nanofibers, especially the fiber diameter and uniform size, can have an influence on the cell adhesion. The fabricated nanofibers with a smaller diameter may have an advantage in being used for application of bone tissue replacement. Other research revealed that differentiation of osteoblast is better for nanofibers with a smaller diameter without beads (Sisson et al. 2010).

Wettability and surface roughness of nanofibers

The nanofibers were further investigated using water contact angle to analyze the surface wettability, which can be a determining factor for cell attachment and adhesion. Table 1 shows that the water contact angle of PCL nanofiber is 132° ± 3.5°, which is in the range of a highly hydrophobic surface or lower wettability. With the addition of nHA, the water contact angle was decreased, proving the successful incorporation of hydrophilic nHA into PCL nanofibers. The chemical structure of nHA is $Ca_5(PO4)_3(OH)$. The hydrophilic OH group causes the lower water contact angle in nHA/PCL membrane.

Table 1 Viscosity of solutions, average fiber diameter and contact angle of PCL and 10% (w/w) nHA/PCL nanofibers

Concentration	0% nHA (w/w)	10% nHA (w/w)
Average fiber diameter (μm)	0.25 ± 0.08	0.65 ± 0.18
Beads	Yes	No
Viscosity (cp)	28.5 ± 0.5	30 ± 0.4
Contact angle (°)	132 ± 3.5	112 ± 3.0

The AFM images of the nanofibers show the average mean roughness (Rms) of two types of nanofibers (Fig. 2). A rougher surface was observed from the AFM images after the incorporation of nHA into the PCL. 10% (w/w) nHA/PCL had higher surface roughness of (611.52 ± 91.25) nm, whereas PCL nanofibers exhibited (449.79 ± 82.85) nm. Thus, nHA had an influence on the increase in the surface roughness of the composite nanofibers. The nanofibers' diameter also affects the surface roughness, where a high surface roughness had been reported with a larger fiber diameter, which is in agreement with this present study (Bianco et al. 2009). The diameter of nanofibers was found to increase with increasing nHA into PCL fibers. The surface roughness increase was also directly proportional to the increase of nHA. Furthermore, a rougher surface is important as it can control the adhesion of osteoblast cells and can mimic the surface roughness found in natural bone (Price et al. 2004). In addition to the incorporation of nHA, the arrangements of nanofiber either in aligned or random orientation can also affect the nanofiber surface roughness value. PCL fibers with an aligned arrangement had a smooth surface (Ahmad et al. 2014). In a random orientation, a higher surface roughness was observed (Dias and Bártolo 2013; Lim et al. 2015).

ATR-FTIR

The synthesized powder (nHA) was investigated under ATR-FTIR. The infrared spectrum of nHA is illustrated in Fig. 3. The sample exhibited absorption bands due to hydroxyl stretch at ~3500 cm^{-1} (Wang et al. 2010). A previous study shows that the hydroxyl group decreases when carbonate content increases (Rehman and Bonfield 1997). The spectrum shows the characteristic of nHA where the intense peak of 1021 cm^{-1} was associated with PO_4^{3-} antisymmetric stretching mode (Paz et al. 2012). The 961 cm^{-1} peak corresponds to the PO_4^{3-}-derived bands (Wang et al. 2010). The peak between 1420 and 1427 cm^{-1} shown in spectrum, at 1348 cm^{-1} and another peak at 826 cm^{-1}, are related to carbonated apatite. The peak at 1560 cm^{-1} refers to the vibrational mode of carbonate ion (Rehman and Bonfield 1997).

On the other hand, in the FTIR spectrum of PCL nanofiber, the peaks at 2867 and 2944 cm^{-1} are associated with asymmetric and symmetric vibrations of the CH_2 group. The C=O vibration of ester at 1721.26 cm^{-1}. The peaks at 1366, 1419, and 1471 cm^{-1} correspond to the CH_2 band vibrations. The ester COO vibrations occur at 1163

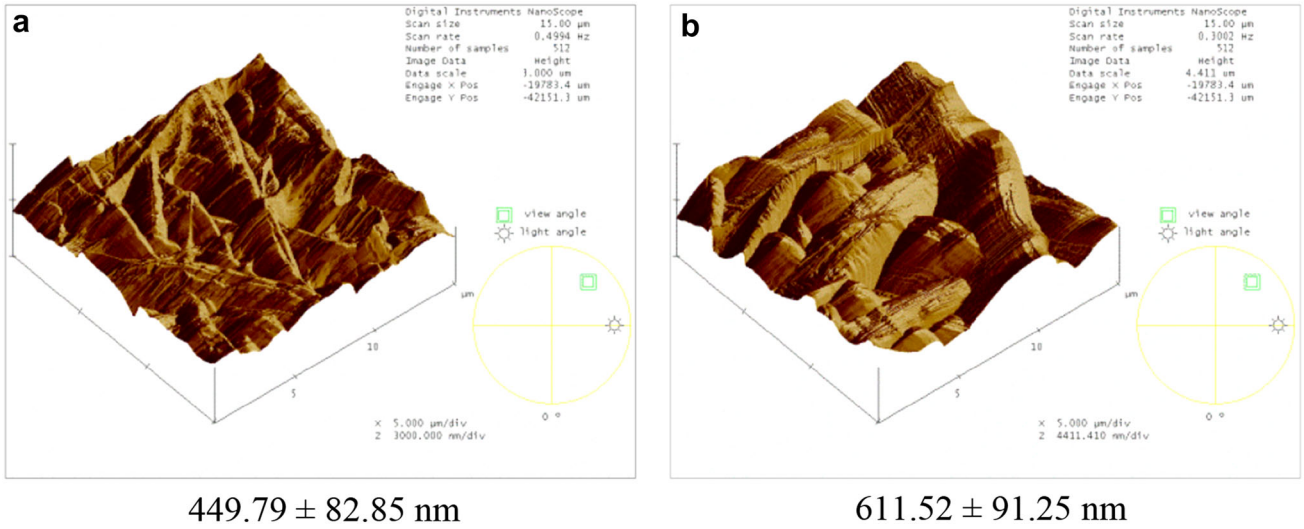

Fig. 2 3D atomic force microscopy (AFM) images of **a** PCL and **b** 10% (w/w) nHA/PCL nanofibers

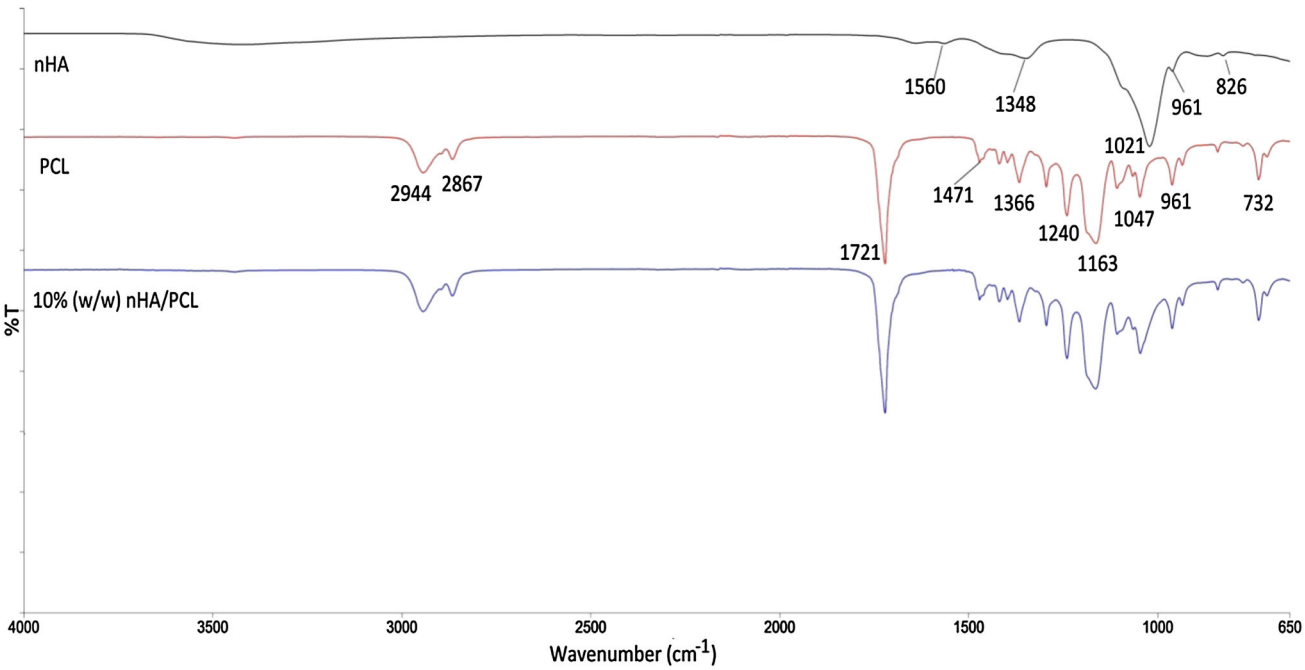

Fig. 3 ATR-FTIR spectra of nHA nanoparticles, PCL and 10% (w/w) nHA/PCL membranes

and 1240 cm^{-1}. The O–C vibrations occur at the peak of 1107, 1047 and 961 cm^{-1}, with the CH_2 vibration appearing at 732 cm^{-1} (Suganya et al. 2011).

The infrared spectrum of PCL nanofibers containing nHA showed almost the same results at all characteristic peaks. With the incorporation of nHA, peak absorption shows only a very small decrease at 1106, 1044, 961 to 732 cm^{-1}. This change confirmed the presence of nHA in the composite nanofibers and the possible interaction of PCL with nHA.

Tensile mechanical properties of fibers

Table 2 shows the ultimate tensile strength and Young's modulus of electrospun PCL and 10% (w/w) nHA/PCL nanofibers calculated from the typical stress–strain curve. Young's modulus was calculated by calculating the slope of the initial linear part of the stress–strain curve, which corresponds to a strain of 8–10% (Fig. 4). From the stress–strain curve of each specimen, the ultimate tensile strength, which is the maximum stress achieved prior to failure, was

calculated. It was observed that the fiber diameter had significant influence on the tensile mechanical properties. Both the modulus and ultimate tensile strength of electrospun PCL fibers were higher than that of 10% (w/w) nHA/PCL electrospun fibers. The higher tensile properties were observed in PCL electrospun fibers, due to their smaller average diameter and uniform fiber diameter as compared to 10% (w/w) nHA/PCL electrospun fibers (Bianco et al. 2009). Lower mechanical properties of PCL nanofibers than nHA/PCL nanofibers were reported (Nirmala et al. 2010). The improvement of the mechanical properties of Young's modulus is due to the smaller fiber diameter and other factors, such as the porosity and orientation of the nanofibers (Bianco et al. 2009). Recently, the mechanical properties of PCL fibers were investigated and it was possible to increase the mechanical properties significantly by coating the fibers using dopamine followed by biomineralization (Xie et al. 2013).

Antibacterial activity and TCH release profile

In order to study antibacterial properties, a membrane with 10% (w/w) nHA/PCL was tested. TCH, a model drug was incorporated in 10% (w/w) nHA/PCL nanofibers. 0.2% TCH is suitable for cell growth since a higher concentration of TCH can be toxic to cells. TCH at a concentration of 0.01 and 0.1 mg/ml is considered good for cell proliferation, and a higher concentration may inhibit the cells' growth (Dashti et al. 2010). The addition of TCH does not affect the morphology of the nanofibers and the water contact angle reduced. To test the feasibility of TCH-loaded 10% (w/w) nHA/PCL electrospun nanofibers, antibacterial activity was tested against Gram-negative *E. coli* and Gram-positive *B. cereus*. Figure 5 shows the performance of the TCH-loaded 10% (w/w) nHA/PCL fibers against *E. coli* and *B. cereus* after 24 h. The diameter of the inhibition zone (clear white zone area) after 24 h proved clear inhibition against the bacteria, with a diameter of inhibition of 2.53 ± 0.06 nm for *E. coli* and 2.87 ± 0.06 cm for *B. cereus*. The diameter of the inhibition zone in *B. cereus* bacteria was greater than that of *E. coli*. This represents the stronger effect of the TCH drug for *B. cereus* compared to *E. coli*. The difference is also due to the factor of the different cell walls' structure of Gram-positive, which contain higher peptidoglycan than Gram-negative bacteria (Augustine et al. 2014). Another study reported the use of TCH with different types of polymers for the treatment of infection in abdominal closure (Hong et al. 2008). Electrospun TCH-loaded 10% (w/w) nHA/PCL nanofibers could be efficient in use against bacterial infection at the bone interface.

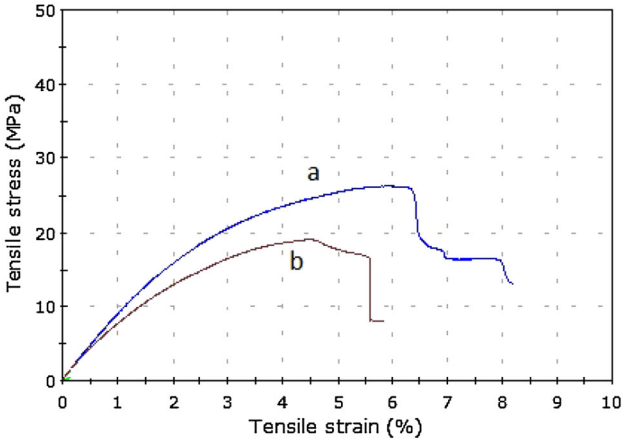

Fig. 4 Tensile stress–strain curves of **a** PCL and **b** 10% (w/w) nHA/PCL membranes

As seen from Fig. 6, it was observed that the TCH/nHA/PCL sample released more TCH in the first week compared to the TCH/PCL nanofibers. However, the release rate of the TCH from TCH/nHA/PCL sample eventually decreased on the 10th day and was nearly equal to the release rate of the TCH/PCL sample. However, the mass of TCH released eventually fluctuated and then went back to nearly the same level on day 23. The TCH/nHA/PCL sample quickly released a large amount of TCH before approaching to the same release rate as the PCL sample. This would indicate that the TCH/nHA/PCL sample would be most suitable to eliminate bacteria within the target region in a short period of time due to the rapid-burst release of a large amount of TCH at the fourth hour. Results from other experiments have also shown that PCL electrospun nanofibers release TCH drugs in short bursts (Mouriño and Boccaccini 2010). The use of TCH/nHA/PCL nanofibers may substitute small bone loss defect and

Table 2 Tensile properties of PCL and 10% (w/w) nHA/PCL nanofiber

Sample	Tensile properties		
	Tensile strain	Young's modulus (MPa)	Ultimate tensile strength (MPa)
10% (w/w) nHA/PCL	4.5 ± 0.5	81.6 ± 1.04	18.5 ± 4.4
PCL	6.4 ± 0.8	88.0 ± 2.04	25.02 ± 2.3

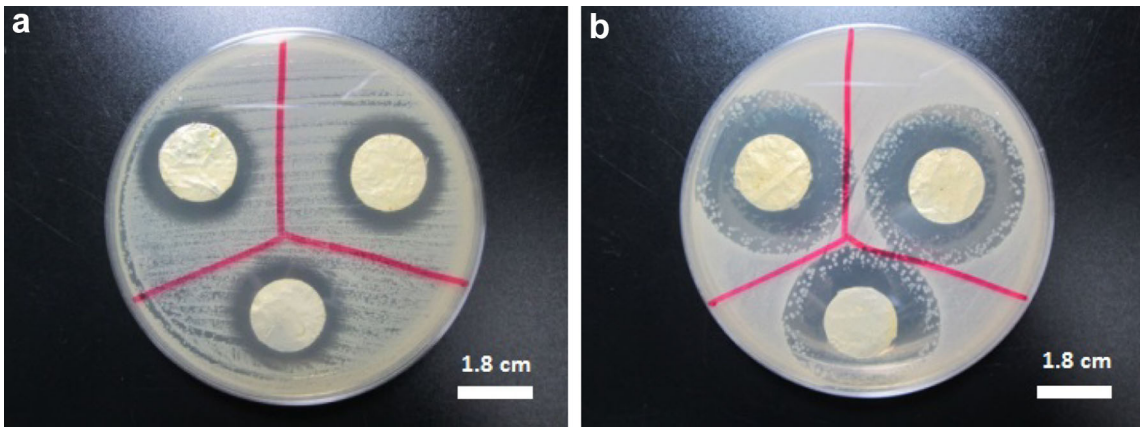

Fig. 5 Antibacterial activity of tetracycline hydrochloride-loaded 10% (w/w) nHA/PCL membranes (triplicate samples); diameter of inhibition zone against **a** *E. coli* (2.53 ± 0.06 cm) and **b** *B. cereus* (2.87 ± 0.06 cm); diameter of nanofibers = 1.8 cm

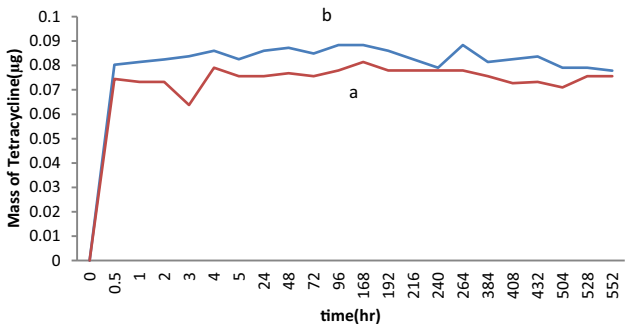

Fig. 6 TCH release profile from **a** PCL and **b** 10% (w/w) nHA/PCL membranes

could eliminate contamination at the local site of bone infection. Besides delivery of TCH, the substitute of bone defect requires important properties, such as osteoconductivity and osteoinductivity. This is achieved by adding nHA and did not hinder the release of TCH, but provided better release.

Conclusions

Incorporation of 10% (w/w) nHA into the PCL membrane using the electrospinning technique produced uniform fiber diameter. The fiber diameter was greatly influenced by the concentration and the viscosity of the solution. The wettability decreased with the incorporation of nHA. The results revealed that 10% (w/w) nHA/PCL nanofibers had higher surface roughness and lower mechanical properties than PCL nanofibers. TCH/nHA/PCL nanofibers possessed antibacterial properties. TCH/nHA/PCL membrane exhibited increased drug release behavior than TCH/PCL membrane.

Acknowledgements The authors would like to acknowledge Muhammad Raihan Abdul Kadir, financial support under FRGS (vote: 4F507), GUP HiCOE grant 4J191 and the facilities provided by FBME, UTM, RMC and MOHE.

References

Agarwal S, Wendorff JH, Greiner A (2009) Progress in the field of electrospinning for tissue engineering applications. Adv Mater 21:3343–3351. doi:10.1002/adma.200803092

Ahmad A, Boggs E, Patel MR et al (2014) Surface modification of electrospun polycaprolactone fibers and effect on cell proliferation. Surf Innov 2:47–59. doi:10.1680/si.13.00018

Augustine R, Malik HN, Singhal DK et al (2014) Electrospun polycaprolactone/ZnO nanocomposite membranes as biomaterials with antibacterial and cell adhesion properties. J Polym Res 21:347. doi:10.1007/s10965-013-0347-6

Bianco A, Di Federico E, Moscatelli I et al (2009) Electrospun poly(ε-caprolactone)/Ca-deficient hydroxyapatite nanohybrids: microstructure, mechanical properties and cell response by murine embryonic stem cells. Mater Sci Eng C 29:2063–2071. doi:10.1016/j.msec.2009.04.004

Chong LH, Lim MM, Sultana N (2015) Fabrication and evaluation of polycaprolactone/gelatin-based electrospun nanofibers with antibacterial properties. J Nanomater 2015:1–8. doi:10.1155/2015/970542 **(Article ID 970542)**

Chung H, Sun T, Sultana N et al (2016) Conductive PEDOT: PSS coated polylactide (PLA) and membranes: fabrication and characterization. Mater Sci Eng C 61:396–409

Dashti A, Ready D, Salih V et al (2010) In vitro antibacterial efficacy of tetracycline hydrochloride adsorbed onto Bio-Oss?? bone graft. J Biomed Mater Res Part B Appl Biomater 93:394–400. doi:10.1002/jbm.b.31594

Davachi SM, Kaffashi B, Torabinejad B et al (2016) Investigating thermal, mechanical and rheological properties of novel antibacterial hybrid nanocomposites based on PLLA/triclosan/nano-hydroxyapatite. Polym (Guildf) 90:232–241. doi:10.1016/j.polymer.2016.03.007

Dias J, Bártolo P (2013) Morphological characteristics of electrospun PCL meshes—the influence of solvent type and concentration. Procedia CIRP 5:216–221. doi:10.1016/j.procir.2013.01.043

Hassan MI, Sultana N, Hamdan S (2014) Bioactivity assessment of poly (ε-caprolactone)/hydroxyapatite electrospun fibers for bone tissue engineering application. J Nanomaterials 2014:573238. doi:10.1155/2014/573238

Hong Y, Fujimoto K, Hashizume R et al (2008) Generating elastic, biodegradable polyurethane/poly(lactide-co-glycolide) fibrous sheets with controlled antibiotic release via two-stream electrospinning. Biomacromol 9:1200–1207. doi:10.1021/bm701201w

Jaiswal AK, Chhabra H, Kadam SS et al (2013) Hardystonite improves biocompatibility and strength of electrospun polycaprolactone nanofibers over hydroxyapatite: a comparative study. Mater Sci Eng C 33:2926–2936. doi:10.1016/j.msec.2013.03.020

Kim CH, Khil MS, Kim HY et al (2006) An improved hydrophilicity via electrospinning for enhanced cell attachment and proliferation. J Biomed Mater Res Part B Appl Biomater 78:283–290

Kim YJ, Park MR, Kim MS, Kwon OH (2012) Polyphenol-loaded polycaprolactone nanofibers for effective growth inhibition of human cancer cells. Mater Chem Phys 133:674–680. doi:10.1016/j.matchemphys.2012.01.050

Koneru B, Shi Y, Wang YC, Chavala SH, Miller ML, Holbert B, Conson M, Ni A, Di Pasqua AJ (2015) Tetracycline-containing MCM-41 mesoporous silica nanoparticles for the treatment of *Escherichia coli*. Molecules 20:19690–19698

Leung V, Ko F (2011) Biomedical applications of nanofibers. Polym Adv Technol 22:350–365. doi:10.1002/pat.1813

Li L, Li G, Jiang J et al (2012) Electrospun fibrous scaffold of hydroxyapatite/poly (ε-caprolactone) for bone regeneration. J Mater Sci Mater Med 23:547–554. doi:10.1007/s10856-011-4495-0

Lim MM, Sun T, Sultana N et al (2015) In vitro biological evaluation of electrospun polycaprolactone/gelatine nanofibrous scaffold for tissue engineering. J Nanomaterials 2015:303426. doi:10.1155/2015/303426

Mouriño V, Boccaccini AR (2010) Bone tissue engineering therapeutics: controlled drug delivery in three-dimensional scaffolds. J R Soc Interface 7:209–227. doi:10.1098/rsif.2009.0379

Nirmala R, Nam KT, Park DK et al (2010) Structural, thermal, mechanical and bioactivity evaluation of silver-loaded bovine bone hydroxyapatite grafted poly(ε-caprolactone) nanofibers via electrospinning. Surf Coat Technol 205:174–181. doi:10.1016/j.surfcoat.2010.06.027

Paz A, Guadarrama D, López M, González JE, Brizuela N, Aragón J (2012) A comparative study of hydroxyapatite nanoparticles synthesized by different routes. Quim Nova 35:1724–1727

Pillay V, Dott C, Choonara YE et al (2013) A review of the effect of processing variables on the fabrication of electrospun nanofibers for drug delivery applications. J Nanomaterials 2013:789289. doi:10.1155/2013/789289

Price RL, Ellison K, Haberstroh KM, Webster TJ (2004) Nanometer surface roughness increases select osteoblast adhesion on carbon nanofiber compacts. J Biomed Mater Res A 70:129–138. doi:10.1002/jbm.a.30073

Putti M, Simonet M, Solberg R, Peters GWM (2015) Electrospinning poly(ε-caprolactone) under controlled environmental conditions: influence on fiber morphology and orientation. Polym (United Kingdom) 63:189–195. doi:10.1016/j.polymer.2015.03.006

Rehman I, Bonfield W (1997) Characterization of hydroxyapatite and carbonated apatite by photo acoustic FTIR spectroscopy. J Mater Sci Mater Med 8:1–4. doi:10.1023/A:1018570213546

Romeo V, Gorrasi G, Vittoria V (2007) Encapsulation and exfoliation of inorganic lamellar fillers into polycaprolactone by electrospinning. Biomacromol 8:3147–3152

Samavedi S, Horton CO, Guelcher SA et al (2011) Acta Biomaterialia fabrication of a model continuously graded co-electrospun mesh for regeneration of the ligament–bone interface. Acta Biomater 7:4131–4138. doi:10.1016/j.actbio.2011.07.008

Sisson K, Zhang C, Farach-Carson MC et al (2010) Fiber diameters control osteoblastic cell migration and differentiation in electrospun gelatin. J Biomed Mater Res Part A 94:1312–1320. doi:10.1002/jbm.a.32756

Suganya S, Senthil Ram T, Lakshmi BS, Giridev VR (2011) Herbal drug incorporated antibacterial nanofibrous mat fabricated by electrospinning: an excellent matrix for wound dressings. J Appl Polym Sci 121:2893–2899. doi:10.1002/app.33915

Sultana N, Wang M (2008) Fabrication of HA/PHBV composite scaffolds through the emulsion freezing/freeze-drying process and characterisation of the scaffolds. J Mater Sci Mater Med 19:2555–2561. doi:10.1007/s10856-007-3214-3

Sultana N, Zainal A (2016) Cellulose acetate electrospun nanofibrous membrane: fabrication, characterization, drug loading and antibacterial properties. Bull Mater Sci 39(2):337–343

Sun B, Long YZ, Zhang HD et al (2014) Advances in three-dimensional nanofibrous macrostructures via electrospinning. Prog Polym Sci 39:862–890. doi:10.1016/j.progpolymsci.2013.06.002

Wang P, Li C, Gong H et al (2010) Effects of synthesis conditions on the morphology of hydroxyapatite nanoparticles produced by wet chemical process. Powder Technol 203:315–321. doi:10.1016/j.powtec.2010.05.023

Webster TJ, Ahn ES (2007) Nanostructured biomaterials for tissue engineering bone. Springer, Berlin

Wutticharoenmongkol P, Sanchavanakit N, Pavasant P, Supaphol P (2006) Preparation and characterization of novel bone scaffolds based on electrospun polycaprolactone fibers filled with nanoparticles. Macromol Biosci 6:70–77. doi:10.1002/mabi.200500150

Wutticharoenmongkol P, Pavasant P, Supaphol P (2007) Osteoblastic phenotype expression of MC3T3-E1 cultured on electrospun polycaprolactone fiber mats filled with hydroxyapatite nanoparticles. Biomacromol 8:2602–2610. doi:10.1021/bm700451p

Xie J, Zhong S, Ma B et al (2013) Controlled biomineralization of electrospun poly(ε-caprolactone) fibers to enhance their mechanical properties. Acta Biomater 9:5698–5707. doi:10.1016/j.actbio.2012.10.042

Zadegan S, Hosainalipour M, Rezaie HR et al (2011) Synthesis and biocompatibility evaluation of cellulose/hydroxyapatite nanocomposite scaffold in 1-n-allyl-3-methylimidazolium chloride. Mater Sci Eng C 31:954–961. doi:10.1016/j.msec.2011.02.021

Zhang Y, Su B, Venugopal J et al (2007) Biomimetic and bioactive nanofibrous scaffolds from electrospun composite nanofibers. Int J Nanomed 1:623–638

Zheng F, Wang S, Shen M et al (2013) Antitumor efficacy of doxorubicin-loaded electrospun nano-hydroxyapatite-poly(lactic-co-glycolic acid) composite nanofibers. Polym Chem 4:933–941. doi:10.1039/C2PY20779F

Zhou WY, Wang M, Cheung WL et al (2008) Synthesis of carbonated hydroxyapatite nanospheres through nanoemulsion. J Mater Sci Mater Med 19:103–110. doi:10.1007/s10856-007-3156-9